NDT&E International 45 (2012) 1–8

Contents lists available at SciVerse ScienceDirect

NDT&E International

journal homepage: www.elsevier.com/locate/ndteint

Nonlinear acoustic characterization of micro-damaged materials through higher harmonic resonance analysis

A. Novak, M. Bentahar*, V. Tournat, R. El Guerjouma, L. Simon

LAUM, CNRS, Université du Maine, Av. O. Messiaen, 72085 Le Mans Cedex 9, France

ARTICLE INFO

Article history:
Received 20 January 2011
Received in revised form
20 August 2011
Accepted 5 September 2011
Available online 14 September 2011

Keywords:
Nonlinear acoustics
Nonlinear resonance
Nonlinear convolution method
Acoustic characterization

ABSTRACT

A method developed for the analysis of nonlinear systems is applied for the first time to non-destructive testing of diverse materials using vibrations and elastic waves. This method allows to extract the vibrational/acoustical responses of the system, at the excitation frequency and importantly, also at higher harmonics, with the help of a nonlinear convolution signal analysis. It is then possible to make use of the robust nonlinear resonance method together with the harmonic generation method in order to analyze the nonlinear elastic resonances of a sample at excitation frequency harmonics. Definitions of the nonlinear hysteretic parameters associated to higher harmonic resonances are provided. The bases of the signal analysis method are also described. A higher sensitivity to the presence of gradual damage compared to the classical nonlinear resonance method is demonstrated experimentally for diverse materials and configurations.

1. Introduction

In the last years, considerable interest has been shown in the study of nonlinear mesoscopic elastic materials or microinhomogeneous materials [1–6]. Rocks, micro-cracked metals, composites, bone, concrete, granular media obey generally to the classical nonlinear theory of elasticity for strain amplitudes corresponding to approximately 10^{-6} and lower. At higher strain amplitudes ($\varepsilon \gtrsim 10^{-6}$), their behavior is no longer adequately described by the classical theory of elasticity [6–9]. It has been found that other types of nonlinearity come into play such as clapping, hysteresis, in the observed nonlinear manifestations. Therefore, different theoretical approaches have been proposed in order to explain the nonclassical experimental observations by considering physical assumptions on the particular features of each one of the aforementioned materials (cracks, internal contacts, friction delaminations…) [3,6,10–12]. Various nonlinear processes have been studied in the context of these nonclassical nonlinearities: nonlinear resonances, harmonic generation, self-demodulation, transfer of modulation, self-action [13–16]. It is often observed that the measurements of nonlinear parameters from these nonlinear processes are more sensitive to the presence of damage than linear elastic parameters (measured through linear acoustic methods), especially at early damage states [17]. With nonlinear resonance experiments, some nonlinear dissipative and nonlinear elastic properties, such as the parameters of hysteretic nonlinearity, are assessed from the downshift of the resonance frequency as well as the diminution of the quality factor with increasing strain amplitude [17–20]. In second harmonic generation experiments, other nonlinear parameters of the material such as the parameter of quadratic nonlinearity are accessible. These two different types of approaches revealed to be interesting non-destructive testing (NDT) tools and allowed the characterization of damage in a wide range of materials. However, in these distinct nonlinear acoustic NDT methods, the signal analysis is performed on a limited range of parameters, where the processes involve some of the nonlinear parameters. In particular, for the widely used nonlinear resonance method, the commonly used gain-phase analyzers measure frequency response functions by comparing input and output signals, only at the frequency of excitation. Information on the nonlinearly generated higher order frequency components is consequently lost.

In this article, we present a damage characterization method which makes use of a suited signal processing for the identification of nonlinear systems, and we apply it to different samples in various experimental configurations. This method can be seen as a coupled nonlinear-resonance/harmonic-generation method, providing access to nonlinear parameters that have not been reported in the literature yet and exhibit a strong dependence on damage. A nonlinear convolution is performed in order to measure simultaneously the linear acoustic frequency response function (FRF) of the material over one or several modes of resonance and the usually out-of-reach higher-order FRF (showing the resonances of the higher harmonic modes) [21]. The amplitude of the latter at the intact state reveals to be weak or nondetectable. However, when materials are damaged,

* Corresponding author.
E-mail address: mourad.bentahar@univ-lemans.fr (M. Bentahar).

0963-8695/$ - see front matter © 2011 Published by Elsevier Ltd.
doi:10.1016/j.ndteint.2011.09.006

we show that harmonic FRF cannot be neglected since they provide sensitive information on damage in terms of their strong amplitude and drive amplitude dependence.

In the first section, we recall the useful principles of nonlinear elasticity of micro-damaged materials. Then, excitation signal and its associated inverse filter implemented in the nonlinear convolution method (NLCM) are presented. Finally, the experimental procedure is described and followed by the sections showing the results, discussion and conclusions.

2. Nonlinear dynamic elasticity: definition of hysteretic parameters

Numerous static and dynamic experiments have shown that the classical theory of nonlinear elasticity is unable to describe the elastic behavior of nonlinear mesoscopic elastic materials [2,22]. In particular, their stress–strain relationship has to be developed in such a way that terms describing hysteresis and discrete memory are taken into account [10]. In this context, the one-dimensional stress–strain relationship can be expressed as

$$\sigma(\varepsilon) = K_0(1+\beta\varepsilon+\delta\varepsilon^2+\cdots)\varepsilon + H[\varepsilon, sign(\dot{\varepsilon})], \quad (1)$$

where σ is the stress, ε is the strain, K_0 is the linear elastic modulus, β and δ represent the classical quadratic and cubic nonlinear parameters, respectively, which can be developed as a combination of second, third and fourth order elastic constants [7,23], H is a function describing the hysteretic relation between σ and ε, and $\dot{\varepsilon}$ is the strain rate [10,22,24–26].

In Eq. (1) classical and hysteretic nonlinear behaviors are clearly differentiated. Indeed, when a material with classical nonlinearity is excited with an acoustic perturbation of frequency ω and strain amplitudes ε_A, it generates higher frequency stress components $2\omega, 3\omega \ldots$ whose amplitudes are proportional to ε_A^2, $\varepsilon_A^3 \ldots$. However, when the material behaves nonlinear hysteretic, amplitudes of odd and even harmonics are seriously disturbed when compared to the classical nonlinear case. For instance, odd harmonics are observed to be of higher amplitudes than even ones and the third harmonic is proportional to ε_A^2 [27], as predicted theoretically [14,20]. For homogeneous solids, polymer composites, it has been observed that they behave, most of the time, linearly when they are not damaged. For the highest excitation levels, they sometimes exhibit classical nonlinearity. When they are damaged, hysteretic nonlinearity becomes detectable in their dynamic behavior. This ensures that methods, which are sensitive to the hysteretic nonlinearity, are well suited for the non-destructive evaluation of initially linear or classically nonlinear media. In standing waves conditions, the main manifestations of the hysteretic nonlinearity are the downward shift of the resonance frequency (corresponding to an elastic modulus softening) and the diminishing of the quality factor of the resonance with increasing excitation amplitude [6,17,19,25].

The function H in Eq. (1) for the dynamic elastic problem is currently under investigation by different research teams. Several models exist for the description of this function. The model of hysteretic quadratic nonlinearity [22,26] provides the opportunity to develop analytical approaches and is sufficiently realistic to explain some of the important manifestations observed in hysteretic materials (downward frequency shift proportional to the strain amplitude, diminution of the quality factor …). For instance, the largely encountered Hertz–Mindlin contact of two elastic spheres, subjected to a shear excitation, is described by the hysteretic quadratic nonlinearity at the leading order of the nonlinear approximation [28]. The phenomenological formulation based on the Preisach–Mayergoyz (PM) theory of hysteresis has also been applied [1,7,8,10,29]. In this approach, the hysteretic nonlinearity comes from discrete hysteretic elastic elements (hysterons), either in the closed state or in the open state, with different characteristic stresses σ_o and σ_c, respectively, for the opening or closing transition. These characteristic stresses are located in the so-called PM space according to a distribution. A given material, taken at a given state, can thus be characterized by a specific PM distribution. It has been shown that when the level of damage for a given sample is increased, the PM distribution is modified, which provides an interesting way to characterize the damage in a material from acoustic experiments. Other models have been proposed, in particular to account for the slow dynamic effects, conditioning and relaxation, frequency dependent effects [30], and are not discussed here.

In most of the experimental observations, the hysteretic nonlinear behavior observed at strain amplitudes above approximately $\varepsilon_A \sim 10^{-6}$ during nonlinear resonance experiments exhibits the same trends [19]. The relative shift in frequency defined as

$$\frac{\Delta f}{f_0} = \frac{f(\varepsilon_A) - f_0}{f_0}, \quad (2)$$

where $f(\varepsilon_A)$ is the resonance frequency at the detected amplitude ε_A and f_0 is the resonance frequency at infinitely low strain amplitude (the linear resonance frequency), is observed proportional to ε_A.

Similarly, the relative change of inverse quality factor:

$$\Delta(1/Q) = \frac{1}{Q_0} - \frac{1}{Q(\varepsilon_A)}, \quad (3)$$

where Q_0 is the quality factor of the resonance at infinitely low strain amplitude and $Q(\varepsilon_A)$, the quality factor at strain amplitude ε_A, is observed proportional to ε_A.

Consequently, two parameters are defined in the literature, corresponding to the proportionality coefficients. The parameter of hysteretic elastic nonlinearity α_f is such that

$$\Delta f/f_0 = -\alpha_f \varepsilon_A \quad (4)$$

and the parameter of hysteretic dissipative nonlinearity α_Q is defined as

$$\Delta(1/Q) = -\alpha_Q \varepsilon_A. \quad (5)$$

The parameters α_f and α_Q measure the importance of hysteretic effects (respectively, elastic and dissipative) in the context of the nonlinear resonance method. The parameter corresponding to the ratio of these two parameters of hysteretic nonlinearity:

$$R = \alpha_Q/\alpha_f \quad (6)$$

is known as the Read parameter [31,32] and compares the importance of the dissipative and elastic hysteretic effects. Note that this parameter is equal to 1 in the approximation of quadratic hysteretic nonlinearity [19]. Note also that this definition of the Read parameter contains some influence from linear properties of the system, and a purely nonlinear Read parameter can be defined as [32]

$$R^{nl} = \frac{2\pi}{Q_0} + R. \quad (7)$$

Obviously, this correction is meaningful only for low quality factors Q_0, i.e. it becomes useless for $RQ_0 \gg 2\pi$. Also, this correction can be of importance when nonlinear parameters are compared for different materials or different damage states with different linear dissipative properties.

In linear resonant systems (plates, bars, rods), there are several modes of resonance that are excited by a monochromatic source when its frequency is tuned to the resonance frequency of the modes. In a nonlinear medium, the initial monochromatic signal can be distorted and new frequencies are generated, themselves

exciting additional resonance modes (harmonic modes). So far, the excitation of harmonic modes has been neglected in the nonlinear resonance experiments because this method focuses on the output information at the initial frequency of excitation, i.e. on the self-action nonlinear process. However, it is expected that additional useful information can be obtained from the excitation of harmonic resonance modes (existence, frequency shift, quality factor decrease…), i.e. a combination of harmonic generation process and nonlinear resonance process. Moreover, in nonlinear resonant systems, there can be some particular situations where the harmonic modes have amplitudes comparable to the mode at the fundamental frequency. In this case, interactions between waves at different frequencies and comparable amplitudes provide nonsimplex interactions [33,34]. For hysteretic media, nonsimplex wave interactions do not exhibit the same trends than simplex (monochromatic) wave interactions such as the resonance frequency shift proportional to the amplitude at the resonance. Consequently, even in the usual way of performing nonlinear resonance experiments, there could be situations where harmonic modes could have a strong influence on the fundamental resonance mode. In an attempt to go further in the understanding of the nonlinear resonances of hysteretic complex materials with NDT&E applications, we define in the following the hysteretic parameters associated to the harmonic resonance modes, which are experimentally accessible through the signal processing method described in the next section.

First, by analogy to the parameter α_f of hysteretic elastic nonlinearity for the fundamental resonance mode, the parameter α_{nf} for the nth harmonic mode is defined as

$$\frac{\Delta f_n}{f_n} = \frac{f_n(\varepsilon_A) - f_{n0}}{f_{n0}} = -\alpha_{nf}\varepsilon_A, \tag{8}$$

where f_n is the resonance frequency of the nth harmonic mode (close to frequency nf) at the fundamental resonance amplitude ε_A and f_{n0} the infinitely low amplitude resonance frequency of the nth harmonic mode. Similarly, for the change in inverse quality factor, we define α_{nQ} as

$$\Delta\left(\frac{1}{Q_n}\right) = \frac{1}{Q_{n0}} - \frac{1}{Q_n(\varepsilon_A)} = -\alpha_{nQ}\varepsilon_A, \tag{9}$$

where Q_n is the quality factor of the nth harmonic mode obtained for a fundamental resonance amplitude ε_A and Q_{n0} the infinitely low amplitude quality factor of the nth harmonic mode. The mathematical procedure used to determine α_{nf} and α_{nQ} for the higher harmonics is the same as for the fundamental component. When a harmonic resonance is observed, its corresponding harmonic resonance frequency $f_n(\varepsilon_A)$ is determined experimentally by picking the frequency of the curve maximum amplitude and the harmonic quality factor $Q_n(\varepsilon_A)$ is determined by the width of the curve at -3 dB from the maximum. Parameters α_{nf} and α_{nf} are then obtained through a linear fit of $\Delta f_n/f_n$ and $\Delta(1/Q_n)$, respectively, as a function of the fundamental amplitude ε_A.

The following equivalent Read parameter is finally defined for the nth harmonic mode:

$$R_n = \frac{\alpha_{nQ}}{\alpha_{nf}}. \tag{10}$$

It should be noticed that the above defined higher order Read parameters R_n have an essential different physical meaning from the one attributed to the fundamental classical Read parameter R (see Eq. (6)). Indeed, it is expected that a complex combination of different nonlinear effects (harmonics generation, self-action, nonsimplex interaction, etc.) contribute to R_n. Accordingly, R_n arise from some nonlinear effective characteristics of the "wave-medium" interaction. In addition, the shape of the FRF in the linear approximation (the sample geometry, boundary conditions, velocity dispersion, sensors positioning, etc.) has a non-negligible influence on the R_n determination.

Depending on the sample geometry, boundary conditions, velocity dispersion, nonlinearity, sensor positions, higher orders are detected or not. This constitute also an important piece of information. In the following, experimental results are presented for three different configurations associated, respectively, to three different types of samples. The hysteretic parameters are obtained for progressively damaged states of the samples. The next section gives the basis of the signal processing method used for the experimental extraction of the previously defined hysteretic parameters α_{nf} and α_{nQ}.

3. Signal processing: the nonlinear convolution method

A usual way to determine the frequency response function (FRF) of a linear system is to use a sine wave with frequency f_{in} and amplitude A_{in} at the input of the system, and to measure the output amplitude A_{out} for different frequencies f_{in}. The FRF can also be obtained much faster using a swept-sine wave with constant amplitude and evaluating the output amplitude as a function of the input swept-sine frequency. Both methods can be used to estimate FRF of linear systems, which are amplitude-independent. However, in the case of identification of nonlinear systems, FRF-based analyzes are not adequate and other signal processing schemes have to be setup.

Indeed, the amplitude-dependence character of a system (nonlinearity) has the obvious consequence that the FRF changes when modifying the amplitude of the excitation signal. This is the case for instance for the nonlinear resonance frequency shift [24,25,19]. Another classical nonlinear effect is the generation of higher harmonics. In that case, the FRF has no more sense, because it is ill-defined. Nevertheless, for practical NDT&E applications, the nonlinear system is usually measured in the same way as for a linear system. In this case, only the transfer of the energy on the first harmonic in the frequency domain can be analyzed.

Among numerous methods for identifying nonlinear systems, the one presented here is based on a method first described in [35], and detailed and extended in [21], in the framework of audio system analysis.

The method uses an exponential swept-sine signal $s(t)$ as an excitation signal and takes into account all the harmonics present in the distorted output signal. The method allows us to estimate the transfer of energy, not only on the first harmonic, but also on higher harmonics. This estimation is realized thanks to the determined harmonic FRFs. The method also allows us to estimate the phase spectra of the harmonic FRFs. Thus, within one single measurement of time length T, the method can characterize the nonlinear system in both amplitude and phase, not only for the fundamental harmonic as usual, but also for nonlinearly generated higher harmonics [21].

The input exponential swept sine signal $s(t)$ (Fig. 1) has an instantaneous frequency $f_i(t)$ which increases exponentially with time, and is defined as

$$s(t) = \sin\left\{2\pi f_1 L\left[\exp\left(\frac{t}{L}\right) - 1\right]\right\}, \tag{11}$$

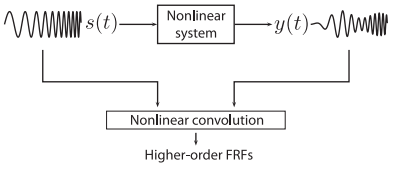

Fig. 1. Block diagram of the nonlinear convolution method.

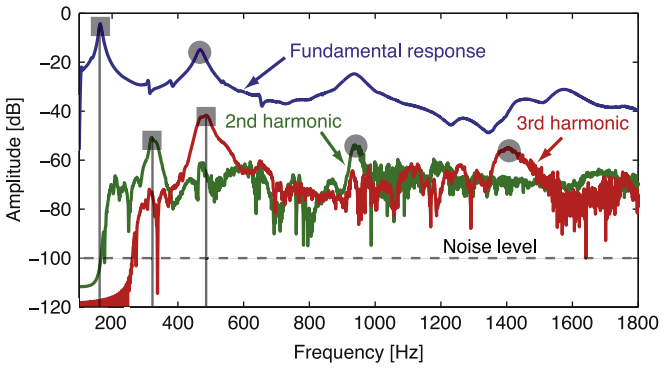

Fig. 2. Result of the nonlinear convolution method in the form of spectra at fundamental, second and third harmonic components. The square and disc symbols show some correspondences in the resonances of the system at fundamental, second and third harmonics. The classical analysis by the method of nonlinear resonances via a spectrum analyzer provides only the curve at the generated fundamental component.

where the rate of exponential increase L is such that

$$L = \frac{1}{f_1}\text{Round}\left(\frac{\hat{T}f_1}{\log\left(\frac{f_2}{f_1}\right)}\right). \tag{12}$$

The properties of the swept sine signal are defined by start and end frequencies f_1 and f_2 and by the approximate time support $\hat{T}$.

The block diagram of the method is depicted in Fig. 1. The analysis procedure is divided into two parts. First, the input swept-sine signal $s(t)$ is generated to excite the nonlinear system whose response $y(t)$ is synchronously recorded. Next, the convolution between the output $y(t)$ and an inverse filter is calculated. The use of the inverse filter in order to separate the higher-order components was proposed in [35] as the time-reversal of the excitation signal, equalized with a slope of -6 dB/oct (time-reversal mirror plus whitening filter). When convolving the output and the inverse filter, the result yields in setting of nonlinear impulse responses. They can be easily separated by windowing and their Fourier Transforms are equal to the higher-order FRFs.

A typical experimental result is shown in Fig. 2 as an illustration. The classical information obtained in a nonlinear resonance experiment at one excitation amplitude corresponds to the curve at the fundamental response. Additional information is contained in the second and third order FRFs. Hysteretic parameters α_{nf} and α_{nQ} are extracted from these higher-order FRFs for different excitation amplitudes. In the next section a set of experimental results is presented, for diverse solids in various configurations, in order to show the adaptability and generality of the developed approach. Finally, it should be pointed out that the results of the presented method would be similar to the ones obtained by a frequency sweep in combination with FFT in a sliding window. However, the use of the nonlinear convolution method ensures several advantages, such as faster measurements, better signal to noise-ratio, and most importantly much better time-frequency resolution since no windowing is applied to the output signal.

4. Experimental results

In the first subsection, the general description of the set-up is given, valid for the three studied samples and configurations. Then in the following subsections, experimental results are presented for three different materials, steel-TiC composite beams, glass rods, and polymer based beams (see Fig. 3).

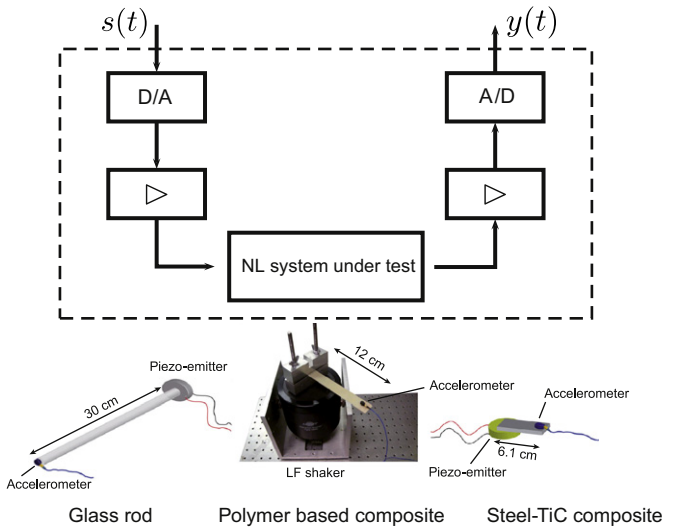

Fig. 3. (top) Block diagram of the experimental configuration for nonlinear convolution method (NLCM) characterization. (bottom) Schematic representation of the three experimental configurations and tested samples (corresponding to the nonlinear systems of the top diagram).

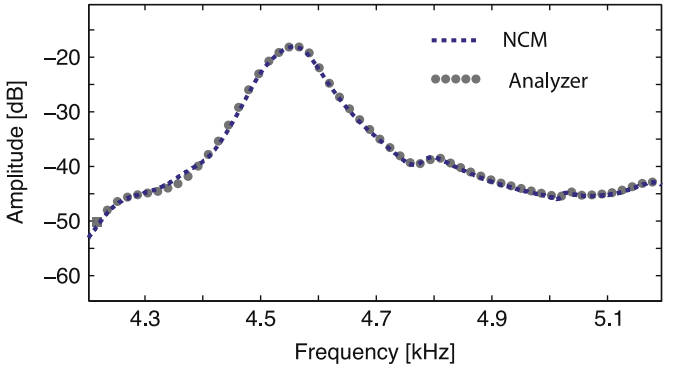

Fig. 4. Comparison between the classical method using a gain-phase analyzer (dots) and the nonlinear convolution method (dashed line) in the vicinity of a resonance of the system.

4.1. Experimental device and linearity study

The schematics of the experimental set-up is presented in Fig. 3. Generation of swept-sine signals is made up using RME Fireface 400 interface. Once amplified at a constant gain, signals excite either piezoceramics or a frequency shaker depending on the required experimental configuration. Vibrations are measured by an accelerometer attached at the free boundary of each sample and connected to a conditioning amplifier. Vibration signals are finally digitized at 24 bits, with a sampling frequency of $f_s = 192$ kHz by the RME Fireface 400 interface before the computer data processing.

As a first stage, the proposed experimental configuration associated to NLCM analysis has been compared to classical resonance experiments in which gain-phase analyzers are generally used [17,19,32]. As depicted in Fig. 4, both results superimpose well, the mean and maximum relative differences between both resonance curves being 0.3% and 2%, respectively.

In order to characterize the linearity of the experimental device we use a material whose nonlinearity is well below the one originating from the electronic devices themselves [6]. Accordingly, we perform NLCM resonance experiments on steel-TiC nanotextured composite material beams of 25% TiC volume fraction. These

metal-based composites are excited with piezoelectric ceramics firmly attached with cyanite glue at one extremity to generate ultrasonic vibrations, which are detected at the other tip with an accelerometer (Fig. 3). The experimental configuration and the sample plate-like geometry ($61 \times 9.5 \times 2.5$ mm) favor the generation of bending resonance modes. Three samples are used as references and are kept at the intact state, while the other ones are damaged using an INSTRON quasi-static tensile machine. All samples are excited around their fundamental bending mode at intact as well as at damaged states using excitations from 1 V to 10 V, corresponding to accelerations at resonance up to 80 m/s^2 at 26 kHz.

For intact samples, NLCM analyzes reveal that the observation of higher harmonics is only possible at the highest acceleration level (80 m/s^2), where an isolated second harmonic appeared at -60 dB (see Fig. 5b). The acceleration level corresponding to 80 m/s^2 can be considered as the nonlinear threshold of the experimental device, not only because of the appearance of a weak second harmonic, but also because the stability of the resonance frequency, as well as the quality factor of this fundamental bending mode, as a function of the driving level has been respected up to 80 m/s^2. Once submitted to the same driving levels, tensile damaged steel-TiC beams show a considerable increase in the second harmonic amplitude from -60 dB to -15 dB (Fig. 5d).

Under these conditions, the proposed experimental device is able to accurately describe the evolution of fundamental and harmonic resonance modes, as a function of driving levels, in the case of two state experiments (damaged and undamaged), and/or gradual damage experiments.

Fig. 5 shows that several parameters can be extracted, such as those defined in Section 2, f_0, Q_0, α_f, α_Q. To be able to extract α_{2f} and α_{2Q} one needs sufficiently well shaped resonances, which is not the case for the poorly detected second harmonic mode of the intact sample (Fig. 5c).

4.2. Glass bar damage characterization: experiments for intact and damaged states

In this second experiment, glass rods of 30 cm long and 1 cm in diameter are firmly attached to a piezoceramic on one end, and resonances are detected using an accelerometer fixed at the other end (Fig. 3). During these experiments, glass samples were only excited around the fundamental compression resonance mode (Young mode). The evolution of the latter as a function of the driving level is first measured at the initial intact state, for excitation levels from 1 V to 10 V, providing a maximum acceleration of 58 m/s^2 ($\varepsilon_A \simeq 2 \times 10^{-7}$). Then, glass samples are locally thermally damaged at a distance of 1/3 the length of the rod from the emitter, and excited at the same previous amplitude and frequency values.

At the intact state, the behavior of the glass samples is typically linear and shows neither frequency nor quality factor significant change with increasing excitation levels. This is visible in Figs. 6 and 7 where relative shifts in resonance frequency and inverse quality factor are difficult to observe. Furthermore, NLCM analyzes show that the only generated higher-order harmonic mode, for the intact state, is the third one, with a very weak amplitude corresponding to -80 dB, at the highest excitation level. With the introduction of damage, the fundamental Young mode resonance shifts from 13.6 kHz (initial state) to 12.3 kHz. This means that, at weak driving levels, the third harmonic

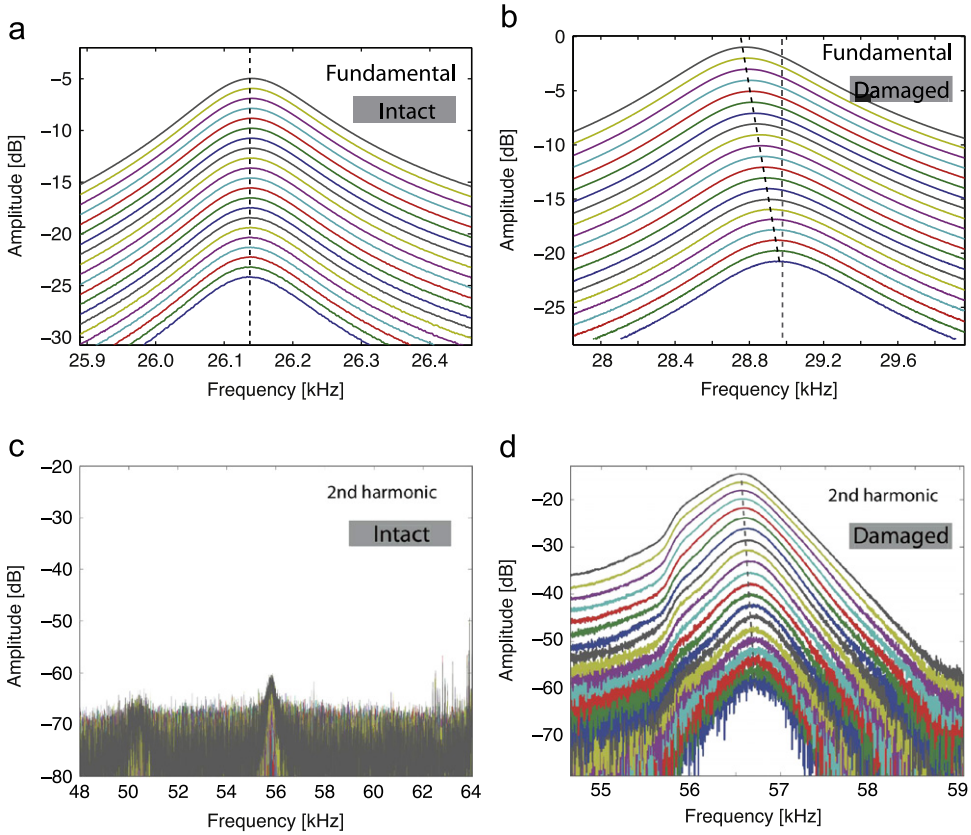

Fig. 5. Spectra obtained by the nonlinear convolution method (NLCM) around the first flexural resonance frequency of the Steel-TiC composite beam. (a) Fundamental response of the intact sample, (b) fundamental response of the damaged sample, (c) second harmonic response of the intact sample, (d) second harmonic response of the damaged sample.

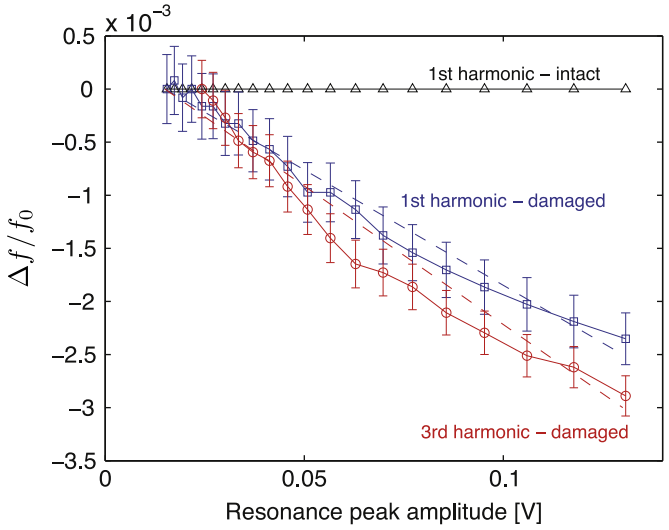

Fig. 6. Relative frequency shift as a function of the detected voltage amplitude at the fundamental resonance, for the fundamental resonance mode at intact and damage states and the third harmonic resonance mode at damage state.

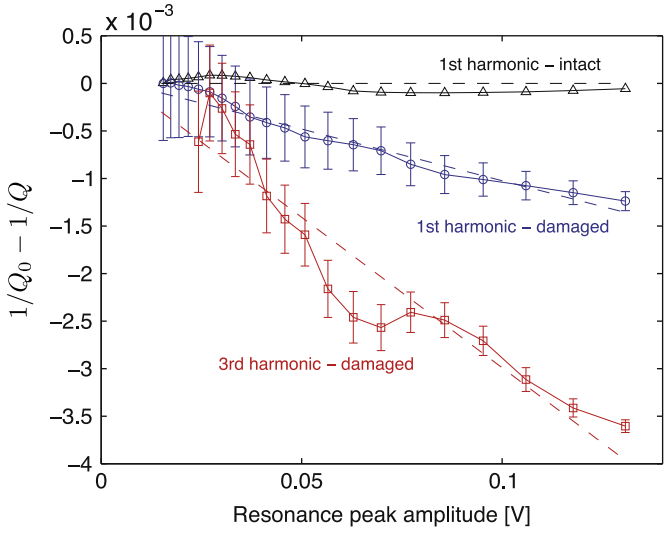

Fig. 7. Relative shift in inverse quality factor as a function of the detected voltage amplitude at the fundamental resonance, for the fundamental resonance mode at intact and damage states and the third harmonic resonance mode at damaged state.

component should be expected around 40.8 kHz and 36.9 kHz for the initial and damaged states, respectively.

For increasing excitations, the nonlinear hysteretic behavior can be appreciated through the hysteretic parameters α_f and α_Q, whose values change from almost zero at the initial intact state up to 1.35×10^4 and 0.65×10^4 at the damaged state. Note that the values of α_f and α_Q given here are obtained by extracting the slopes of the curves shown in Figs. 6 and 7, where the resonance peak amplitude is expressed in terms of strain amplitude (0.13 V detected amplitude corresponds to $\varepsilon_A\simeq2\times10^{-7}$).

Moreover, with introduced damage, the third harmonic increases considerably by more than 30 dB for the same excitation levels, with an absence of any other odd and even harmonics. The analysis of this third harmonic, whose observation is impossible when using usual gain-phase analyzers, shows an interesting behavior. Indeed, α_{3f} (third harmonic frequency hysteretic parameter) is slightly higher than α_f ($\alpha_{3f}\simeq1.65\times10^4$), while the hysteretic parameter α_{3Q} (third harmonic quality factor hysteretic parameter) is much higher than α_Q ($\alpha_{3Q}=2\times10^4$). The sensitivity to damage detection of this new α_{3Q} parameter is then better than the α_Q parameter.

The joint evolution of α_{nf} and α_{nQ} with damage ($n=1,3$) can be followed through the Read factor R_n defined in Section 2: $R_1\simeq0.48$ and $R_3\simeq1.2$. These results show that, while damping evolution is twice less than frequency evolution for the fundamental mode, the third harmonic exhibits more balanced activities.

Finally, Fig. 7 shows a nonmonotonous behavior of the quantity $\Delta(1/Q_3)$ as a function of the resonance peak amplitude. It deviates from the model assumption which is a linear decrease with strain amplitude. This point will be discussed later in this article.

4.3. Polymer-based sample characterization: gradual damage experiments

For this last experiment, the composite is a glass fiber reinforced polyester resin, where two symmetric four plies $[90/0_2]_s$ are used. The composite plate is gradually damaged with a classical three point bending technique. Damage steps are induced within the same sample at step-off levels going from 0 to 3 mm in 1 mm increments. Resonance experiments are carried out on the same sample in order to follow the effect of the increasing damage on the excited resonance bending modes. In a concern to be close to the real composite resonances, we used a low weight B&K accelerometer (1 g), positioned at half of the cantilever end deflection. Contrary to glass bars and Steel-TiC plates, we detect a non-negligible second harmonic of the first resonance bending mode even at the intact state. At the maximum excitation level, the second harmonic resonance peak is at -40 dB while the amplitude of the fundamental mode is at -4 dB. Furthermore, the intact cross-ply composite exhibits a nonlinear hysteretic behavior observed with increasing driving level. The obtained set of fundamental resonance curves, provides the following hysteretic parameters $\alpha'_f=1.47\times10^{-2}$ and $\alpha'_Q=2.47\times10^{-2}$ (see Table 1) at the non damaged state 0. Due to the difficulty in relating the detected acceleration to the actual strain ε_A in the beam excited on its flexural modes, we denote with a prime the hysteretic parameters α'_f and α'_Q that correspond to the slopes of the relative frequency shift $\Delta f/f_0$ and relative change in inverse quality factor $\Delta(1/Q)$, respectively, as a function of the detected electrical amplitude. Yet, there is proportionality with α_f and α_Q, and the relative modifications of these parameters which are discussed in the following are the same.

It should be noticed that α'_f does not change significantly as a function of the induced damage since its maximum variation, between state 0 and state 3, is around 2. Simultaneously, α'_{2f} which is comparable to α'_f at the intact as well as the first damage state, increases clearly at the damage states 2 and 3 and becomes approximately three times α'_f at the final state. The parameter α'_Q remains roughly unchanged at intact as well as damaged states.

Table 1
Evolution of hysteretic parameters α'_f, α'_Q, α'_{nf}, α'_{nQ} of the polymer-based composite as a function of damage level.

Damage states	α'_f	α'_Q
State 0	$(1.47\pm0.23)\times10^{-2}$	$(2.47\pm0.06)\times10^{-2}$
State 1	$(1.61\pm0.18)\times10^{-2}$	$(2.68\pm0.16)\times10^{-2}$
State 2	$(2.32\pm0.23)\times10^{-2}$	$(1.96\pm0.23)\times10^{-2}$
State 3	$(3.12\pm0.38)\times10^{-2}$	$(2.64\pm0.29)\times10^{-2}$
Damage states	α'_{2f}	α'_{2Q}
State 0	$(1.12\pm0.46)\times10^{-2}$	$(0.5\pm0.9)\times10^{-2}$
State 1	$(1.16\pm0.56)\times10^{-2}$	$(2.48\pm1.50)\times10^{-2}$
State 2	$(2.64\pm0.62)\times10^{-2}$	$(4.04\pm0.64)\times10^{-2}$
State 3	$(10.20\pm1.91)\times10^{-2}$	$(11.91\pm1.98)\times10^{-2}$

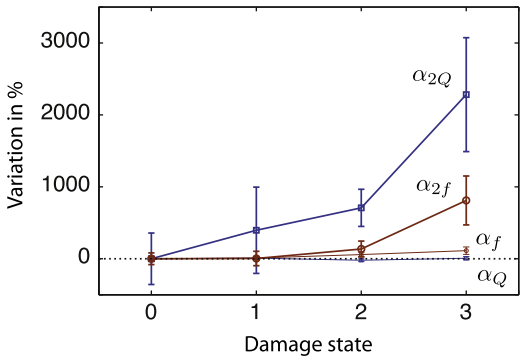

Fig. 8. Relative variations of the parameters α_{nf} and α_{nQ} as a function of damage level. The sensitivity to damage for the parameters α_{2f} and α_{2Q} obtained by the NLCM method is much higher than for existing classical hysteretic parameters.

Table 2
Evolution of Read factor corresponding to the fundamental (R_1) as well as second harmonic (R_2) as a function of increasing damage in the polymer-based composite.

Read factors	State 0	State 1	State 2	State 3
R_1	1.68	1.66	0.84	0.84
R_2	0.44	2.13	1.53	1.16

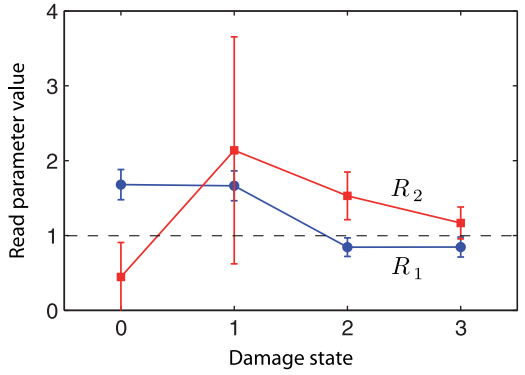

Fig. 9. Evolution of the Read factors R_1 and R_2 as a function of damage in the polymer-based composite.

However α'_{2Q} whose value is nine times less than α'_Q at the intact state increases strongly (25 times approximately) with damage (see Fig. 8).

Values of Read factors R_n for $n=1$ and $n=2$ are obtained using the above values of the parameters α'_f, α'_Q, α'_{2f}, α'_{2Q}, as shown in Table 2. For R_1, a noticeable transition from $R_1>1$ (nonlinear hysteretic dissipation is dominant) to $R_1<1$ (nonlinear hysteretic elasticity is dominant) is observed as a function of increasing damage. Actually this trend is fully explained by the above described variations on α_f and α_Q with damage. Simultaneously, the behavior of R_2 does not exhibit the same trend. Indeed, a nonmonotonous dependence on damage is observed (see Fig. 9), and this makes any systematic conclusion difficult or even non-realistic, at the present time. However, the encouraging fact in this new observation is that R_2 has a non-negligible dynamics as a function of damage. In that sense, further dynamic experiments are necessary to assess the use of R_2 as a reliable structural health monitoring (SHM) parameter.

5. Discussion and conclusions

The above presented experimental results correspond to three various configurations and samples. In all the observations, a higher sensitivity of the newly accessible parameters α_{nf} and α_{nQ} (thanks to the adapted nonlinear convolution method) compared to the conventional ones α_f and α_Q is demonstrated. It is particularly clear in Fig. 8 where the evolution of the higher order hysteretic parameters can be more than 10 times faster than first order hysteretic parameters as a function of the level of damage. This observation could lead to earlier detection of damage using nonlinear acoustic methods.

The higher order sensitivity joins the results found in [36,37], where higher order interactions are considered in the case of the elastic modulation approach applied on cracked samples. In both contributions, authors proposed the clapping Hertzian nonlinearity as a model to describe the nonlinear behavior of samples with crack-like defects. In the present work, the physical mechanisms at the origin of the existing harmonic resonances, which are extracted thanks to the nonlinear convolution method, have not been analyzed. The nonlinear generation of the corresponding frequencies can in principle originate from all the nonlinear terms of Eq. (1), quadratic, cubic or hysteretic. However, one might expect the sensitivity of the proposed nonlinear characterization method to be reduced in the case of disadvantageous damage interaction with the generated acoustic stress (or strain) field (damage is near the stress nodes). Furthermore, the boundary conditions and the dispersive character of the resonance modes are expected to play roles in the detection of harmonic modes. Consequently, the measured higher order hysteretic parameters depend in general on the quadratic, cubic and hysteretic nonlinearity of the medium (supposed to be correlated to damage [6,17]) but also on the linear dispersive and attenuation properties of the material, the boundary conditions, and the detector position. Further work on the amplitude dependence of higher order modes for instance could lead to discriminate the dominant involved processes.

The evolution of the relative change in inverse quality factor for the higher harmonics is sometimes observed to be non monotonous, as shown in Fig. 7. This behavior has not been considered in the definition of the associated new hysteretic parameters α_{nf} and α_{nQ}. Such behavior may be explained by the nonsimplex (or complex) nonlinear hysteretic interactions of waves [33,34]. When the strain signal in the medium is composed of several frequencies (is nonsimplex), there are frequency and amplitude combinations that lead to various possible observations for the nonlinear resonances. In particular, a nonmonotonous behavior in the relative frequency shift or in the relative change of inverse quality factor is predicted when the relative amplitudes of the different frequency components change. This is an interesting point for further studies from the theoretical and experimental point of view.

In the frame of a pure hysteretic effect, Read factor has already been determined by considering different hysteretic models (Granato–Lücke breakaway hysteresis, Davidenko hysteresis, etc.), where the differences in the determined values have not been so drastic [38]. However, it should be pointed out that for microinhomogeneous materials, in which the concentration of defects is not too small, it has been found that hysteretic nonlinearity (related to adhesion and friction effects) acts simultaneously with some nonhysteretic mechanisms (e.g. thermoelastic losses at crack mating faces, where the loss magnitude is strongly dependent on geometry of defects) [39,30]. Therefore, one should be careful in using directly R to diagnose the hysteresis type [39]. In the light of the aforementioned works, we can still follow simultaneously the evolution of both α_{nf} and α_{nQ} for increasing damage through Read factors R_n ($n\geq 1$). In that case, we can find that R_1 and R_2 do not have the same dynamics. R_1 decreases by approximately 50% in a step-like way resembling to a triggering phenomenon. This bi-state behavior could be

explained by the fact that, at each damage step, the material releases a given amount of its elastic energy. At a certain cumulative energy value, released when moving from state 1 to state 2 in our case, R_1 becomes suddenly less than one (~ 0.84) and remains constant for increasing damage (state 3). However, R_2 is nonmonotonous for increasing damage as observed in Fig. 9. To our knowledge this is the first study of R_2 to be undertaken on microinhomogeneous materials as a function of gradually increasing damage. In order to draw a definitive conclusion about the way R_2 and R_1 change with damage, we still need higher number of calibrated damage states to confirm the evolution of Read factors as a function of the elastic energy (where damage mechanisms could be considered together and/or separately) released at every damage state. In fine, energetic quantification of damage will offer a new way to observe changes induced in R_1 and R_2, and in higher order resonances as well R_n ($n \geq 3$), with a consequent wealth on SHM applications.

Finally, the reported nonlinear convolution method which consists of a coupled nonlinear-resonance/harmonic-generation method allows further developments already deeply studied in the context of the classical nonlinear resonance method. For instance, slow dynamics monitoring as well as conditioning for harmonic resonance modes could be studied and may also exhibit a higher sensitivity to damage than the classical nonlinear resonance method.

Acknowledgements

This work was supported by the project AMETIS (Advanced Metallurgical Technologies for Innovative Systems).

References

[1] Guyer R, Johnson P. Nonlinear mesoscopic elasticity: evidence for a new class of materials. Phys Today 1999;52:30–6.
[2] Naugolnykh K, Ostrovsky L. Nonlinear wave processes in acoustics, Cambridge texts in applied mathematics. Cambridge University Press; 1998.
[3] Ostrovsky L, Johnson P. Dynamic nonlinear elasticity in geomaterials. Riv Nuovo Cimento 2001;24:1–46.
[4] Cate JT, Smith E, Guyer R. Universal slow dynamic in granular solids. Phys Rev Lett 2000;85:1020–3.
[5] Tournat V, Zaitsev V, Nazarov V, Gusev V, Castagnède B. Experimental study of nonlinear acoustic effects in a granular medium. Acoust Phys 2005;51(5):543–53.
[6] Bentahar M, El Aqra H, El Guerjouma R, Griffa M, Scalerandi M. Hysteretic elasticity in damaged concrete: quantitative analysis of slow and fast dynamics. Phys Rev B 2006;73:014116.1–10.
[7] Landau L, Lifshitz E. Theory of elasticity. New York: Pergamon; 1986.
[8] Abeele KVD, Visscher JD. Damage assessment in reinforced concrete using spectral and temporal nonlinear vibration techniques. Cem Concr Res 2000;30:1453–64.
[9] Renaud G, Calle S, Remenieras J, Defontaine M. Exploration of trabecular bone nonlinear elasticity using time-of-flight modulation. IEEE Trans Ultrason Ferroelectr Freq Control 2008;55(7):1497–507.
[10] Guyer R, McCall K, Boitnott N. Hysteresis, discrete memory and nonlinear wave propagation in rock: a new paradigm. Phys Rev Lett 1995;74(17):3491–4.
[11] Scalerandi M, Delsanto P, Agostini V, Abeele KVD, Johnson P. Local interaction simulation approach to modeling nonclassical, nonlinear elastic behavior in solids. J Acoust Soc Am 2003;113:3049–59.
[12] Zaitsev V, Gusev V, Castagnède B. Thermoelastic mechanism for logarithmic slow dynamics and memory in elastic wave interaction with individual cracks. Phys Rev Lett 2003;90:075501.1–4.
[13] Cantrell J, Yost W. Acoustic harmonic generation from fatigue induces dislocation dipoles. Philos Mag A 1994;69:315–26.
[14] Abeele KVD, Johnson P, Sutin A. Nonlinear elastic wave spectroscopy (NEWS) techniques to discern material damage. Part I: nonlinear wave modulation spectroscopy. Res Nondestr Eval 2000;12(1):17–30.
[15] Moussatov A, Castagnède B, Gusev V. Frequency up-conversion and frequency down-conversion of acoustic waves in damaged materials. Phys Lett A 2002;301:281–90.
[16] Zaitsev V, Nazarov V, Tournat V, Gusev V, Castagnède B. Luxembourg–Gorky effect in a granular medium: probing perturbations of the material state via cross-modulation of elastic waves. Europhys Lett 2005;70(5):607–13.
[17] Bentahar M, El Guerjouma R. Monitoring progressive damage in polymer-based composite using nonlinear dynamics and acoustic emission. J Acoust Soc Am 2009;125(1):EL39–44.
[18] Muller M, Sutin A, Guyer R, Talmant M, Laugier P, Johnson P. Nonlinear resonant ultrasound spectroscopy (NRUS) applied to damage assessment in bone. J Acoust Soc Am 2005;118(6):3946–52.
[19] Johnson P, Sutin A. Slow dynamics and anomalous nonlinear fast dynamics in diverse solids. J Acoust Soc Am 2005;117(1):124–30.
[20] Abeele KVD, Carmeliet J, Cate JT, Johnson P. Nonlinear elastic wave spectroscopy (NEWS) techniques to discern material damage. Part II: Single mode nonlinear resonance acoustic spectroscopy. Res Nondestr Eval 2000;12(1):31–42.
[21] Novak A, Simon L, Kadlec F, Lotton P. Nonlinear system identification using exponential swept-sine signal. IEEE Trans Instrum Meas 2010;59(8):2220–9.
[22] Guyer R, Johnson P. Nonlinear mesoscopic elasticity. Wiley-VCH; 2009.
[23] Hamilton MF, Blackstock D. Nonlinear acoustics. San diego: Academic Press; 1998.
[24] Holcomb D. Memory, relaxation, and microfracturing in dilatant rock. J Geophys Res 1981;86:6235–48.
[25] Nazarov V, Ostrovsky L, Soustova I, Sutin A. Nonlinear acoustics of micro-inhomogeneous media. Phys Earth Planet Inter 1988;50(1):65–73.
[26] Gusev V. Parametric acoustic source in a medium with hysteretic quadratic non-linearity. Acoust Lett 1998;22:30–4.
[27] Meegan G, Johnson P, Guyer R, McCall K. Observations of nonlinear elastic wave behavior in sandstone. J Acoust Soc Am 1993;94(6):3387–91.
[28] Tournat V, Gusev V. Acoustics of unconsolidated "model" granular media: an overview of recent results and several open problems. Acta Acustica United Acustica 2009;96:208–24.
[29] Van Den Abeele K. Multi-mode nonlinear resonance ultrasound spectroscopy for defect imaging: an analytical approach for the one-dimensional case. J Acoust Soc Am 2007;122(1):73–90.
[30] Gusev V, Tournat V. Amplitude- and frequency-dependent nonlinearities in the presence of thermally-induced transitions in the Preisach model of acoustic hysteresis. Phys Rev B 2005;72:054104.
[31] Read TA. The internal friction of single metal crystals. Phys Rev 1940;58:371–80.
[32] Inserra C, Tournat V, Gusev V. Characterization of granular compaction by nonlinear acoustic resonance method. Appl Phys Lett 2008;92:191916.
[33] Aleshin V, Gusev V, Zaitsev V. Propagation of acoustics waves of nonsimplex form in a material with hysteretic quadratic nonlinearity: analysis and numerical simulations. J Comput Acoust 2004;12(3):319–54.
[34] Zaitsev V, Gusev V, Zaytsev Y. Mutually induced variations in dissipation and elasticity for oscillations in hysteretic materials: non-simplex interaction regimes. Ultrasonics 2005;43(8):699–709.
[35] Farina A. Nonlinear convolution: a new approach for the auralization of distorting systems. In: AES 108th convention. Amsterdam; 2001.
[36] Zaitsev VY, Matveev L, Matveyev AL. On the ultimate sensitivity of nonlinear modulation method of crack detection. NDTE Int 2009;42:622–9.
[37] Zaitsev VY, Matveev L, Matveyev AL. Elastic wave modulation approach to crack detection: comparison of conventional modulation and higher-order interactions. NDTE Int 2011;44:21–31.
[38] Lebedev AB. Amplitude dependent elastic-modulus defect in the main dislocation-hysteresis models. Russ Phys Solid state 1999;41(7):1105–11.
[39] Zaitsev VY, Matveev L. Strain-amplitude dependent dissipation in linearly dissipative and nonlinear elastic microinhomogeneous media. Russ Geol Geophys 2006;47(5):695–710.